A Section 508–conformant HTML version of this article is available at https://doi.org/10.1289/EHP8044.

An Examination of National Cancer Risk Based on Monitored Hazardous Air Pollutants

Chelsea A. Weitekamp,[1] McKayla Lein,[1,2] Madeleine Strum,[3] Mark Morris,[4] Ted Palma,[4] Darcie Smith,[4] Lukas Kerr,[1,2] and Michael J. Stewart[1]

[1]Center for Public Health and Environmental Assessment, Office of Research and Development, U.S. Environmental Protection Agency (U.S. EPA), Research Triangle Park, North Carolina, USA
[2]Oak Ridge Associated Universities, Oak Ridge, Tennessee, USA
[3]Air Quality Assessment Division, Office of Air Quality Planning and Standards, U.S. EPA, Research Triangle Park, North Carolina, USA
[4]Health and Environmental Impacts Division, Office of Air Quality Planning and Standards, U.S. EPA, Research Triangle Park, North Carolina, USA

Background: Hazardous air pollutants, or air toxics, are pollutants known to cause cancer or other serious health effects. Nationwide cancer risk from these pollutants is estimated by the U.S. EPA National Air Toxics Assessment. However, these model estimates are limited to the totality of the emissions inventory used as inputs, and further, they cannot be used to examine spatial and temporal trends in cancer risk from hazardous air pollutants.

Objectives: To complement model estimates of nationwide cancer risk, we examined trends in cancer risk using monitoring data from 2013 to 2017 across the 27 U.S. National Air Toxics Trends Stations.

Methods: For each monitoring site, we estimated cancer risk by multiplying the annual concentration for each monitored pollutant by its corresponding unit risk estimate. We examined the 5-y average (2013–2017) cancer risk across sites and the population levels and demographics within 1-mi of the monitors, as well as changes in estimated cancer risk over time. Finally, we examined changes in individual pollutant concentrations and their patterns of covariance.

Results: We found that the total estimated cancer risk is higher for urban vs. rural sites, with the risk at seven urban sites (of 21) above 75 in 1 million. Furthermore, while most pollutant concentrations have not changed over the time period explored, we found 38 site-pollutant combinations that significantly declined and 12 that significantly increased between 2013 and 2017. We also identified a positive correlation between estimated cancer risk and percent of the population within 1-mi of a monitor that is low income.

Discussion: Long-term trends show that annual mean concentrations of most measured air toxics have declined. Our evaluation of a more recent snapshot in time finds that most pollutant concentrations have not changed from 2013 to 2017. This analysis of cancer risk based on monitored values provides an important complement to modeled nationwide cancer risk estimates and can further inform future approaches to mitigate risk from exposure to hazardous air pollutants. https://doi.org/10.1289/EHP8044

Introduction

Hazardous air pollutants (HAPs), also referred to as air toxics, are air pollutants known or suspected to cause cancer or other serious health effects (U.S. EPA 2020e). There are currently 187 HAPs listed under Section 112 of the Clean Air Act. These pollutants comprise four classes based on the method by which they are measured: carbonyls, volatile organic compounds (VOCs), polycyclic aromatic hydrocarbons (PAHs), and inorganic metals and metalloids [speciated from particulate matter (PM)] (U.S. EPA 2016). Anthropogenic sources of HAPs include mobile sources (e.g., vehicles), relatively large stationary sources (e.g., factories, refineries, power plants), and small area sources (e.g., gas stations, dry cleaners). HAPs also arise from natural sources, such as wildfires or biogenic VOC emissions (U.S. EPA 2018d).

Estimates for nationwide cancer risk from HAPs are reported in the U.S. EPA National Air Toxics Assessment (NATA), typically released in a 3–4 y cycle (U.S. EPA 2018e). These estimations start with the compilation of a national emissions inventory of outdoor air toxics sources for a particular year. Air quality models then estimate average ambient concentrations across the United States, which are used in an exposure model based on time–activity patterns to estimate potential cancer and chronic noncancer public health risks at the census tract level (U.S. EPA 2018e). For the calculation of cancer risk, the estimated exposure concentration is multiplied by the inhalation unit risk estimate for that carcinogen, an upper-bound estimate of an individual's probability of contracting cancer over a lifetime of exposure to 1 $\mu g/m^3$ HAPs in air. Assuming additivity of risk, estimated total cancer risk is equal to the sum of the individual cancer risks from all HAPs to which a person is exposed (U.S. EPA 2018e). Results at the census tract level can be aggregated up to the county, state, or national level. NATA, therefore, provides a snapshot in time of cancer (as well as chronic noncancer) risk from HAPs on a variety of spatial scales.

There are important limitations, however, to consider when interpreting NATA results. For example, as with any exposure model, the accuracy of the risk estimates is highly dependent on the quality and totality of the emissions used as model inputs, and this emissions completeness can vary regionally (Stewart et al. 2019). Given that emissions estimates can vary according to where and when they were produced, NATA documentation explicitly states that the assessments should not be used to compare risks between states, nor to examine trends between years (U.S. EPA 2018e).

To further inform public health risk, some HAP concentrations are routinely monitored throughout the United States, with several hundred monitors that are managed by states, local agencies, and tribes (Strum and Scheffe 2016; U.S. EPA 2018f). However, given that monitoring is typically used to measure ambient concentrations of HAPs associated with a local source (e.g., emissions associated with a pulp and paper mill), the specific HAPs measured at these sites varies (Strum and Scheffe 2016).

Address correspondence to Michael J. Stewart, 109 T.W. Alexander Dr., Durham, NC 27709 USA. Email: stewart.michael@epa.gov

Supplemental Material is available online (https://doi.org/10.1289/EHP8044).

The authors declare they have no actual or potential competing financial interests.

Received 6 August 2020; Revised 26 January 2021; Accepted 12 February 2021; Published 24 March 2021.

Note to readers with disabilities: *EHP* strives to ensure that all journal content is accessible to all readers. However, some figures and Supplemental Material published in *EHP* articles may not conform to 508 standards due to the complexity of the information being presented. If you need assistance accessing journal content, please contact ehponline@niehs.nih.gov. Our staff will work with you to assess and meet your accessibility needs within 3 working days.

Thus, the number of monitored HAPs, the monitoring frequency, and the sampling methodology employed often vary across sites. This limits the ability to directly compare concentrations across monitors. In addition to the locally run monitors, the U.S. EPA monitors ambient levels of HAPs at National Air Toxics Trends Stations (NATTS). These stations use standardized methods and analyses to monitor a core group of 19 HAPs, with a total of 60 HAPs that are suggested to be monitored when possible (U.S. EPA 2016, 2019b). Until 2018, there were 21 urban and 6 rural NATTS (U.S. EPA 2016). Most monitors are located in or near residential areas. A calculation of cancer risk based on monitored HAP concentrations is informative, because in many cases, it allows for a comparison of spatial and temporal trends in cancer risk. Estimating cancer risk based on these ambiently monitored carcinogenic HAP concentrations is not routine; thus this analysis offers a novel complement to the public health information that NATA provides when estimating cancer risk based on modeled concentrations of HAPs for a single year.

Using monitored HAPs data, the 2020 U.S. EPA report "Our Nation's Air" shows generally declining trends for HAP ambient concentrations from 2003 to 2017 (U.S. EPA 2020c). However, trends in cancer risk from HAP concentrations have not been recently examined. Analysis based on cancer risk weights the chemicals driving potential cancer risk and can point to priority pollutants for which a reduction in emissions would have the greatest impact. Here, expanding on previous studies of cancer risk trends from HAPs across years (McCarthy et al. 2009; Strum and Scheffe 2016), we apply novel analyses to examine NATTS monitoring data from 2013 to 2017 across the 27 U.S. sites. Using the 5-y annual average, we estimate total cancer risk from monitored HAPs at each site and assess the relative contribution from VOCs, PAHs, and PM-speciated metals and metalloids. Further, we conduct an analysis of population levels and demographics associated with estimated cancer risk. Next, we examine spatial and temporal trends across sites and HAPs, as well as HAP patterns of covariance. Finally, we directly compare NATA census tract modeled cancer risk estimates to those at NATTS monitors located in the same census tract and for the same year.

Methods

Quality Filtering and Data Preparation

Analyses and figures were generated using R (version 3.4.3; R Development Core Team). R scripts used to process data and generate figures are available on GitHub (https://github.com/USEPA/NATTS-HAP).

For HAP, annual average ambient monitoring data for 2013 to 2017 were obtained from the most recent version of the U.S. EPA Phase XIII Ambient Monitoring Archive (U.S. EPA 2020b). Updates to the archive occur every 1–2 y. Before release of the archived data, the U.S. EPA conducts quality assurance and reduction to ensure standardization and completeness of the reported data (U.S. EPA 2020a). Annual means within the archive were computed from daily averages using two different approaches: *a*) averaging the daily averages, treating nondetects as zeroes and *b*) treating the nondetects as censored values, and using the regression on order statistics (ROS) approach via the nondetects and data analysis (NADA) package in R to compute the means. We compared these means as a criterion for data inclusion and quality assurance. If the ratio of the means (approach 2:approach 1) was greater than 1.3 for a site–pollutant–year concentration, it was assumed that the nondetects (ND) data affect the annual average, and therefore we removed that site–pollutant–year combination (see Table 1 for percent included). This approach is the same one that was used for the 2014 NATA model validation (U.S. EPA 2018e), identified as allowing the greatest number of monitors to be used while avoiding values that may be overly influenced by ND data. Finally, if more than 80% of the values used to compute an annual mean were ND, we used 0 as the annual mean. Following the filtering methodology just described, means used in further analyses were

Table 1. For all national air toxics trends stations from 2013 to 2017, the total number of hazardous air pollutants (HAPs) monitored with unit risk estimates and the percent of those that met our data inclusion criterion.

	Total number of HAPs monitored with unit risk estimates					% satisfying data inclusion criterion				
NATTS	2013	2014	2015	2016	2017	2013	2014	2015	2016	2017
Atlanta, GA	19	35	35	35	37	100%	94%	91%	86%	92%
Bountiful, UT	40	40	39	40	40	98%	90%	97%	90%	85%
Bronx, NY	39	39	39	39	39	97%	95%	92%	95%	97%
Chesterfield, SC	36	33	33	29	33	94%	100%	97%	90%	91%
Chicago, IL	40	40	39	40	40	90%	88%	97%	98%	90%
Detroit, MI	40	40	39	40	40	98%	98%	97%	100%	100%
Grand Junction, CO	40	40	39	40	40	98%	95%	97%	93%	93%
Grayson Lake, KY	40	40	39	40	40	90%	90%	90%	93%	98%
Horicon, WI	35	35	35	35	35	94%	89%	97%	91%	91%
Houston, TX	32	32	32	32	32	100%	94%	100%	94%	97%
Karnack, TX	32	32	32	32	32	94%	84%	94%	94%	94%
La Grande, OR	37	36	36	36	36	97%	100%	94%	83%	86%
Los Angeles, CA	35	35	34	32	35	97%	100%	100%	100%	97%
Phoenix, AZ	40	40	39	40	40	93%	93%	97%	90%	95%
Pinellas County, FL	38	38	38	38	38	97%	100%	100%	100%	100%
Portland, OR	37	37	37	NA	35	97%	95%	89%	NA	94%
Providence, RI	37	37	37	39	39	97%	92%	100%	97%	92%
Richmond, VA	41	41	41	40	40	98%	98%	98%	100%	98%
Rochester, NY	39	39	39	39	39	92%	92%	90%	100%	90%
Roxbury, MA	37	37	37	39	39	95%	92%	97%	92%	95%
Rubidoux, CA	35	35	34	32	35	100%	97%	100%	97%	100%
San Jose, CA	34	34	34	34	35	100%	100%	97%	100%	97%
Seattle, WA	40	40	39	40	40	100%	100%	100%	100%	100%
St. Louis, MO	41	40	39	40	40	95%	90%	95%	98%	95%
Tampa, FL	38	38	38	38	38	100%	97%	97%	100%	97%
Underhill, VT	40	39	39	39	40	95%	90%	82%	87%	95%
Washington, DC	39	39	39	39	39	95%	100%	95%	95%	92%

from the ROS approach. For concentrations of specific HAP metals, we used the annual means from speciated particulate matter with aerodynamic diameter less than or equal to 10 μm (PM_{10}) in our analysis, because PM_{10} measurements include fine particulate matter with aerodynamic diameter less than or equal to 2.5 μm ($PM_{2.5}$) and had a smaller percent of data reported as below the method detection limit (MDL) or ND compared with $PM_{2.5}$ alone (data included after filtering are shown in Excel Table S1).

To promote standardization of monitoring methods and to explore a set of sites across representative areas of the country and a set of well-defined pollutants, we used only monitoring data from NATTS locations and included only chemicals for which there was a unit risk estimate (URE; Table 2). Note that due to an identified discordance in concentrations of ethylene dibromide at co-located monitors, as well as general high rates of erroneous measurements, we excluded this HAP from our analyses. In addition, ethylene oxide monitoring at NATTS sites started in 2019; thus measurements were not available in our data set. Although NATTS monitors aim to measure a common core group of chemicals, the number of chemicals they measure varies across sites and years (see Table 1).

In each of the following cases, data were combined for analysis. The two sites at Grand Junction, Colorado, measured different HAPs and were co-located ($\sim$200 ft apart). In addition, there were several location changes for NATTS between 2013 and 2017. In 2017, the site at La Grande, Oregon (latitude 45.338972, longitude −118.094497), moved approximately 1.3 mi to La Grande Hall (latitude 45.3235, longitude −118.0778). The site is simply referred to as La Grande in this analysis. In 2016, the site at Portland, Oregon, moved approximately 0.3 mi (latitude 45.56137, longitude −122.6679 to latitude 45.558081, longitude −122.670985).

To calculate cancer risk from individual HAPs, we multiplied the unit risk estimate by the annual mean concentration from the monitoring data described above. UREs were obtained from the set of acute and chronic dose–response values compiled by the U.S. EPA Office of Air Quality and Planning Standards and used in the U.S. EPA Human Exposure Model (Table 2) (U.S. EPA 2018a). UREs are derived by the U.S. EPA from the slope of the cancer dose–response curve, which is estimated using a linearized multistage statistical model based on the low-dose region of the curve (U.S. EPA 2018e). These estimates represent a plausible upper limit to the true value and are intended to be health protective. Note, cancer is a collection of diseases that develop through changes in cells and tissues over time (U.S. EPA 2005). Cancer dose–response assessments can be based on tumor incidence data, as well as measures of key precursor events that are part of the carcinogenic process (U.S. EPA 2005). Thus, though cancer is not a single disease, it is treated as such for the purpose of deriving dose–response values.

Trends at NATTS

We used the most recent 5-y averages at the time of analysis (2013–2017) of HAP concentrations to estimate cancer risk. For each site, we calculated the 5-y average cancer risk from monitored HAP by summing the 5-y means of cancer risk for individual HAP. Note, there were missing data for some HAP-site-year combinations. Some HAP were either removed at the filtering stage described above or not reported in the ambient monitoring archive (see Excel Table S2 for a breakdown of HAP included by site and year). For this analysis, we used all available data, including if data meeting our inclusion criteria were available for fewer than 5 y [e.g., if annual average data were available for a given HAP for only two of the 5 y with cancer risks of x and y, the 5-y average was taken as $(x+y)/2$].

To visualize spatial trends in cancer risk associated with HAP concentrations, geospatial analysis was done in Python 3.8.1 (Python Software Foundation) with libraries basemap and matplotlib. Pie charts were created by grouping individual HAPs by their classification (carbonyl, VOC, PAH, or PM-speciated metal/metalloid) using the 5-y average data. The size of the pie charts across sites varies in accordance with total cancer risk at each site (5-y average). To further examine spatial trends across sites, we created a stacked bar plot. For each site, the top ten HAPs with the highest contribution to cancer risk at that site are shown, as well as an "other" group that pooled all other HAPs. To test whether total cancer risk differed between urban and rural sites, we used a Welch two sample t-test ($\alpha \leq 0.05$). The designation of a site as urban or rural was determined by the local air quality agency that operates that site (U.S. EPA 2019a). Urban sites are intended to allow an assessment of the range of population exposures across urban areas. Rural sites are intended to allow for the characterization of exposure of nonurban populations and background concentrations (U.S. EPA 2016). For example, a rural site may be used to measure HAP concentrations outside of a metropolitan statistical area.

To estimate the number of people exposed, we used ArcGIS Pro (10.4, Esri) to examine population levels within a 0.25-, 0.5-, and 1- mi radius from each NATTS monitor. Population values were based on the U.S. Census Bureau 2010 data set (U.S. Census Bureau 2010). Populations for census blocks within the specified distances were joined to the monitor sites if the block centroid was within the given distance of the monitor. The finest resolution of demographic data available was at the census block group level, downloaded from U.S. EPA EJSCREEN. We used the 2019 EJSCREEN data, based on the 5-y American Community Survey from the Census Bureau, which was for years 2013–2017 (U.S. EPA 2019c). For this demographic analysis, we included data for all persons living in block groups where the block group's population-weighted center falls within the 1-mi radius of a NATTS monitor (QGIS 3.16). Three rural sites (Chesterfield, South Carolina; Grayson Lake, Kentucky; and Karnack, Texas) did not have population-weighted census block group centroids within 1-mi of the monitor and therefore were not included in this analysis. Using an average across block groups for each site, we conducted linear regression to examine potential relationships between two demographic variables, percent of the population that is low income (where the household income is less than or equal to twice the federal "poverty level") and percent of the population that is minority status (racial status as a race other than White alone and/or ethnicity as Hispanic or Latino), and the 5-y average estimates of cancer risk in 1 million from monitored HAPs (U.S. EPA 2019c). Because the American Community Survey data represent a 5-y estimate (2013–2017), the federal poverty thresholds correspond to the year of data input (U.S. Census Bureau 2020a, 2020b).

To visually examine temporal trends, we created a time series of total cancer risk change over time (relative to 2013 values), which was calculated using only chemicals that were measured and which met the data inclusion criterion outlined above for all 5 y within a given site (see Excel Table S3 for included chemicals). To examine whether these changes over time were statistically significant, we calculated Spearman's rank correlation coefficients (R version 3.4.3). Finally, to determine whether there were statistically significant changes in cancer risk from individual HAPs over the 5-y period, we calculated Spearman's rank correlation coefficients for individual HAPs at all sites. For this analysis, we included only pollutants measured in at least 30% of sites (8 sites), resulting in analysis for 32 HAPs. For Spearman's rank correlations, a significance level of 0.05, uncorrected for Type I error, was used as the criterion of statistical significance.

Table 2. Carcinogenic hazardous air pollutants monitored at national air toxics trends stations with their associated inhalation unit risk estimate (URE), class, and the top three sources of cancer risk based on the source groups reported for pollutants modeled in the 2014 National Air Toxics Assessment (U.S. EPA 2018a, 2018b).

Hazardous air pollutant	CAS number	URE ($1/(\mu g/m^3)$)	Class	Top three U.S. sources from 2014 NATA based on contribution to national risk
1,1,2-trichloroethane**	79-00-5	1.6×10^{-5}	VOC	Stationary point; oil and gas operations; waste disposal
1,1-dichloroethane	75-34-3	1.6×10^{-6}	VOC	Waste disposal; stationary point; oil and gas operations
1,3-butadiene*	106-99-0	3.0×10^{-5}	VOC	On-road light duty nondiesel vehicles (starts); on-road light-duty nondiesel vehicles (running); residential wood combustion
2-chloro-1,3-butadiene	126-99-8	4.8×10^{-4}	VOC	Stationary point; nonpoint industrial; nonpoint bulk terminals, petroleum, organic, and inorganic chemical storage and transport
9h-fluorene**,#	86-73-7	4.8×10^{-5}	PAH/POM	Fires (sum of prescribed, wild and agricultural); residential wood combustion; on-road light-duty nondiesel vehicles (running)
acenaphthene**,#	83-32-9	4.8×10^{-5}	PAH/POM	Fires (sum of prescribed, wild and agricultural); residential wood combustion; on-road light-duty nondiesel vehicles (running)
acenaphthylene**,#	208-96-8	4.8×10^{-5}	PAH/POM	Fires (sum of prescribed, wild and agricultural); residential wood combustion; on-road light-duty nondiesel vehicles (running)
acetaldehyde*	75-07-0	2.2×10^{-6}	Carbonyl	Secondary; biogenics; on-road light duty nondiesel vehicles (starts)
acrylonitrile**	107-13-1	6.8×10^{-5}	VOC	Stationary point; waste disposal; nonpoint industrial
alpha-chlorotoluene	100-44-7	4.9×10^{-5}	VOC	Stationary point; nonpoint fuel combustion; waste disposal
arsenic*	7440-38-2	0.0043	metal/metalloid	On-road light-duty nondiesel vehicles (running); nonpoint fuel combustion; nonpoint industrial
benzene*	71-43-2	7.8×10^{-6}	VOC	On-road light-duty nondiesel vehicles (starts); on-road light-duty nondiesel vehicles (running); residential wood combustion;
benzo(*a*)anthracene**,#	56-55-3	9.6×10^{-5}	PAH/POM	Fires (sum of prescribed, wild and agricultural); residential wood combustion; on-road light-duty nondiesel vehicles (running)
benzo(*a*)pyrene*,#	50-32-8	0.00096	PAH/POM	Fires (sum of prescribed, wild and agricultural); residential wood combustion; on-road light-duty nondiesel vehicles (running)
benzo(*b*)fluoranthene**,#	205-99-2	9.6×10^{-5}	PAH/POM	Fires (sum of prescribed, wild and agricultural); residential wood combustion; on-road light duty nondiesel vehicles (running)
benzo(*e*)pyrene**,#	192-97-2	4.8×10^{-5}	PAH/POM	Fires (sum of prescribed, wild and agricultural); residential wood combustion; on-road light-duty nondiesel vehicles (running)
benzo[*ghi*]perylene#	191-24-2	4.8×10^{-5}	PAH/POM	Fires (sum of prescribed, wild and agricultural); residential wood combustion; on-road light-duty nondiesel vehicles (running)
benzo(k)fluoranthene**,#	207-08-9	9.6×10^{-6}	PAH/POM	Fires (sum of prescribed, wild and agricultural); residential wood combustion; on-road light-duty nondiesel vehicles (running)
beryllium*	7440-41-7	0.0024	metal/metalloid	Nonpoint fuel combustion; stationary point; locomotives
cadmium*	7440-43-9	0.0018	metal/metalloid	Nonpoint fuel combustion; stationary point; locomotives
carbon tetrachloride*	56-23-5	6.0×10^{-6}	VOC	Background (global contribution), stationary point; waste disposal
chrysene**,#	218-01-9	9.6×10^{-7}	PAH/POM	Fires (sum of prescribed, wild and agricultural); residential wood combustion; on-road light-duty nondiesel vehicles (running)
cis-1,3,-dichloropropene**	10061-01-5	4.0×10^{-6}	VOC	Solvents and coatings; stationary point; oil and gas operations
coronene#	191-07-1	4.8×10^{-5}	PAH/POM	Fires (sum of prescribed, wild and agricultural); residential wood combustion; on-road light-duty nondiesel vehicles (running)
dibenzo[a,h]anthracene**,#	53-70-3	0.00096	PAH/POM	Fires (sum of prescribed, wild and agricultural); residential wood combustion; on-road light-duty nondiesel vehicles (running)
ethylbenzene**	100-41-4	2.5×10^{-6}	VOC	On-road light-duty nondiesel vehicles (starts); on-road light-duty nondiesel vehicles (running); nonroad recreational including pleasure craft
ethylene dichloride	107-06-2	2.65×10^{-5}	VOC	Commercial cooking; stationary point; nonpoint industrial
fluoranthene**,#	206-44-0	4.8×10^{-5}	PAH/POM	Fires (sum of prescribed, wild and agricultural); residential wood combustion; on-road light-duty nondiesel vehicles (running)
formaldehyde*	50-00-0	1.3×10^{-5}	Carbonyl	Secondary; biogenics; fires (sum of prescribed, wild and agricultural)
hexachloro-1,3-butadiene**	87-68-3	2.2×10^{-5}	VOC	Stationary point; waste disposal
hexavalent chromium**	18540-29-9	0.012	metal/metalloid	Stationary point; nonpoint industrial; nonpoint fuel combustion
indeno[1,2,3-*cd*]pyrene**,#	193-39-5	9.6×10^{-5}	PAH/POM	Fires (sum of prescribed, wild and agricultural); residential wood combustion; on-road light-duty nondiesel vehicles (running)
methyl tert-butyl ether**	1634-04-4	2.6×10^{-7}	VOC	Stationary point; waste disposal; nonpoint fuel combustion
methylene chloride**	75-09-2	1.6×10^{-8}	VOC	Solvents and coatings; stationary point; waste disposal
naphthalene*	91-20-3	3.4×10^{-5}	PAH	Solvents and coatings; fires (sum of prescribed, wild, and agricultural); on-road light-duty nondiesel vehicles (starts)
nickel*	7440-02-0	0.00048	metal/metalloid	Stationary point; on-road light-duty nondiesel vehicles (running); fuel combustion
p-dichlorobenzene**	106-46-7	1.1×10^{-5}	VOC	Solvents and coatings; stationary point; agricultural livestock
perylene#	198-55-0	4.8×10^{-5}	PAH/POM	Fires (sum of prescribed, wild and agricultural); residential wood combustion; on-road light-duty nondiesel vehicles (running)
tetrachloroethylene*	127-18-4	2.6×10^{-7}	VOC	Solvents and coatings; stationary point; waste disposal
trans-1,3-dichloropropene**	10061-02-6	4.0×10^{-6}	VOC	Solvents and coatings; stationary point; oil and gas operations
tribromomethane	75-25-2	1.1×10^{-6}	VOC	Stationary point; fuel combustion
trichloroethylene*	79-01-6	4.8×10^{-6}	VOC	Stationary point; solvents and coatings; waste disposal
vinyl chloride*	75-01-4	8.8×10^{-6}	VOC	Stationary point; waste disposal; nonpoint industrial

Note: Many hazardous air pollutants have several synonyms; the names used here reflect those reported at NATTS. NATTS, National Air Toxics Trends Stations; PAH/POM, polycyclic aromatic hydrocarbon/polycyclic organic matter; VOC, volatile organic compound. *NATTS "core" analyte (Tier I). **NATTS principal analyte (Tier II).
#Sources based on risk reported for grouped PAHs/POMs.

Covariance Patterns between HAP Concentrations

To examine whether patterns of covariance differ between rural and urban sites, we created clustered correlation matrices using the 5-y average concentration data for HAPs. Only pollutants that were measured at more than 75% of sites (i.e., fewer than 25% missing values) were included in the analysis. Missing values were imputed using the R package MICE: multivariate imputation by chained equations. Pollutants with 80% or more ND (zeros at all sites) were discarded. To generate heat maps, we used R packages ggplot2 and pvclust. Data were clustered using the complete linkage method and correlation was used as the distance metric.

Comparison with Modeled Cancer Risk Estimates at the Census Tract

To compare the 2014 NATA census tract modeled cancer risk estimates to those based on measured concentrations at NATTS monitors in 2014, we first obtained the NATA cancer risk at the census tracts containing a NATTS monitor by entering the latitude and longitude of the NATTS monitors into the NATA web map application (U.S. EPA 2018b). (Formaldehyde concentrations at the Atlanta, Georgia, NATTS monitor were not reported in the monitoring archive for 2014.) Because the cancer risk estimates produced by NATA are based on exposure concentrations, rather than ambient concentrations, we sought to assess whether differences between the monitored and modeled estimates may be reflective of adjustments from the exposure model used in NATA. Given that formaldehyde is a primary driver of cancer risk, as a case study we examined differences between 2014 NATA exposure and ambient concentrations at the census tract and 2014 NATTS concentrations measured at the monitor. Exposure and ambient formaldehyde concentrations estimated by NATA were obtained by matching the NATTS census tract code (U.S. EPA 2018c).

Results

Spatial Trends

Figure 1 shows the spatial distribution of estimated cancer risk at the 27 NATTS across the United States, apportioned across the four classes of HAPs (classed based on monitoring method; Table S1). The 2013–2017 average cancer risk estimated from monitored HAP concentrations ranged from approximately 24 in 1 million to greater than 100 in 1 million at these sites. (Estimated cancer risk results are rounded to whole numbers in the text.) Estimated cancer risk was primarily driven by monitored carbonyl concentrations (formaldehyde and acetaldehyde), which represented 37%–82% of the cancer risk across these sites. VOCs represented 12%–41%, PAHs represented 1%–11%, and PM-speciated metals and metalloids represented 2%–15% of the estimated cancer risk across NATTS sites.

To examine the relative contributions from individual carcinogenic HAPs at NATTS sites, we created stacked bar plots showing total estimated cancer risk and the top 10 contributing HAP for each site (Figure 2; Excel Table S4). The total estimated cancer risk (5-y annual average) for most sites exceeded 50 in 1 million ($n = 18$; Figure 2), and all sites had an estimated cancer risk greater than 20 in 1 million. Seven urban sites exceeded 75 in 1 million cancer risk. One urban site, Bountiful, Utah, had a 5-y annual average cancer risk estimate greater than 100 in 1 million (Figure 2). When comparing urban and rural monitoring locations, estimated cancer risk was significantly higher in urban sites ($t = 3.23$, $p = 0.011$) with a mean of 67 in 1 million, compared with 42 in 1 million for rural sites. For urban locations, estimated cancer risk ranged from 32 in 1 million to greater than 100 in 1 million, whereas in rural locations, with the exception of Chesterfield, South Carolina, cancer risk estimates were less than 50 in 1 million (Figure 2). For HAPs that were monitored in at least half the sites, the primary drivers of cancer risk at urban sites were formaldehyde, benzene, and acetaldehyde, whereas for rural sites the main drivers were formaldehyde, benzene, and carbon tetrachloride.

To better characterize the potential for cancer risk, we examined population levels within a 0.25-, 0.5-, and 1-mi radius corresponding to the location of the NATTS monitors (Figure 3A; Table S2). When compared across cancer risk ranges (0–25, 26–50, 51–75, 76–100, 101+ per 1 million), we found that a cancer risk of 51–75 in 1 million was associated with the highest population living within a 1-mi radius (Figure 3B; Table S3). The cancer risk group associated with the next largest group of people living within

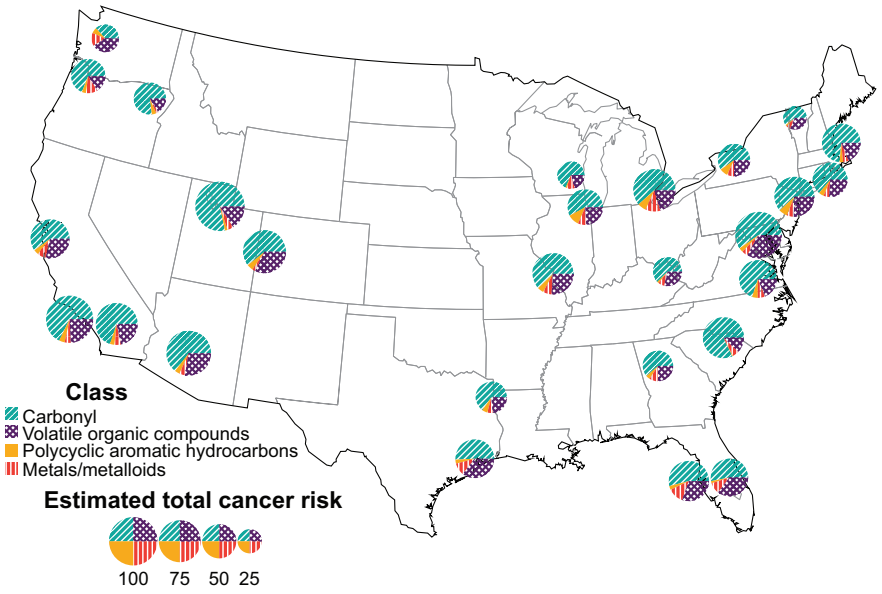

Figure 1. Spatial distribution of National Air Toxics Trends Stations using 2013–2017 annual average data. Composition of pie charts at each site shows percent risk contribution from carbonyls, VOCs, PAHs, and metals/metalloids. The size of each pie chart is continuous and corresponds to the estimated 5-y average total cancer risk in 1 million for that site. Summary data are shown in Table S1. Note: PAHs, polycyclic aromatic hydrocarbons; VOCs, volatile organic compounds.

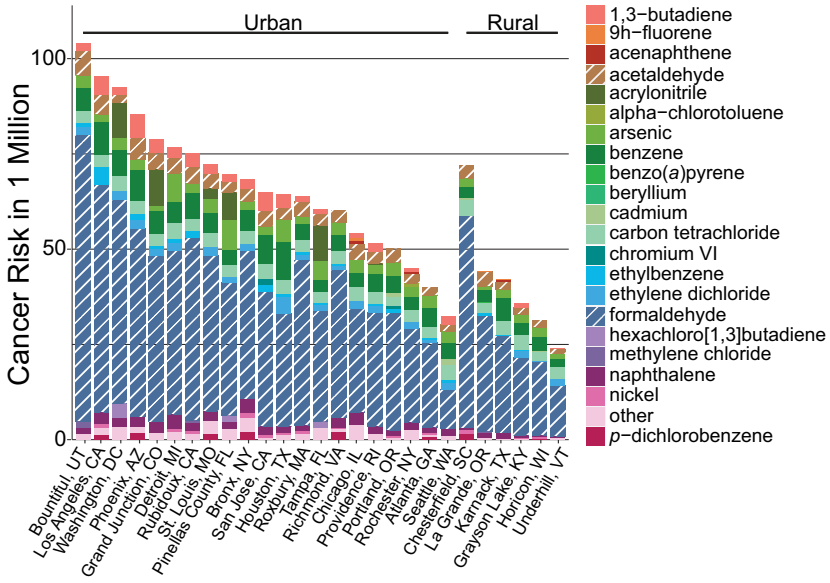

Figure 2. Total estimated cancer risk in 1 million from monitored hazardous air pollutants for every National Air Toxics Trends Stations based on 2013–2017 annual average data. The stacked bar for each site shows the contribution from each of the top 10 pollutants at that site to total cancer risk. Summary data are shown in Excel Table S4.

a 1-mi radius was 76–100 in 1 million (Figure 3B; Table S3). Finally, using linear regression, we found a positive correlation between estimated cancer risk and percent of the population within 1 mi that was low income ($R^2 = 0.13$, $p = 0.04$; Figure 4) and no relationship with percent of the population within 1 mi that was minority status ($R^2 = 0.04$, $p = 0.19$; Figure 4; Table S4).

Temporal Trends

To identify trends in estimated cancer risk from 2013 to 2017, we plotted cancer risk for these years at each NATTS. In general, there was little variation in total cancer risk from 2013 to 2017 (Figure 5; Table S5). In accordance, no sites showed statistically significant ($p < 0.05$) changes in total cancer risk. However, four sites showed trends of decreasing risk, including Bountiful ($\rho = -0.9$, $p = 0.083$), Grand Junction, Colorado ($\rho = -0.9$, $p = 0.083$), Los Angeles, California ($\rho = -0.9$, $p = 0.083$), and Roxbury, Massachusetts ($\rho = -0.9$, $p = 0.083$), where estimated cancer risk decreased from 130 in 1 million to 73 in 1 million, 117 in 1 million to 56 in 1 million, 94 in 1 million to 89 in 1 million, and 70 in 1 million to 48 in 1 million, respectively. In addition, there were notable peaks in cancer risk at three sites, where the change from 2013 was more than 1.5-fold. In Washington, DC, cancer risk peaked at 126 in 1 million in 2015; in Pinellas County, Florida, cancer risk peaked at 95 in 1 million in 2016; and in Chesterfield, cancer risk was 99 in 1 million in 2015 and 83 in 1 million in 2016 (Figure 5; Table S5).

We then examined individual pollutant concentrations over the 5-y period using Spearman's rank correlation coefficients. Most correlation coefficients were not significant (Figure 6; Excel Table S5). Of the 50 site-chemical combinations, 12 had statistically significant ($p < 0.05$) increasing concentrations over time. In Atlanta, 7 PAHs significantly increased, including benzo(*a*)anthracene, benzo(*a*)pyrene, benzo(*b*)fluoranthene, benzo(*e*)pyrene, benzo[*ghi*]perylene, benzo(*k*)fluoranthene, and indeno[1,2,3-*cd*]pyrene. The PAH perylene increased at both Richmond, Virginia, and Seattle, Washington. Finally, arsenic in Phoenix, Arizona,

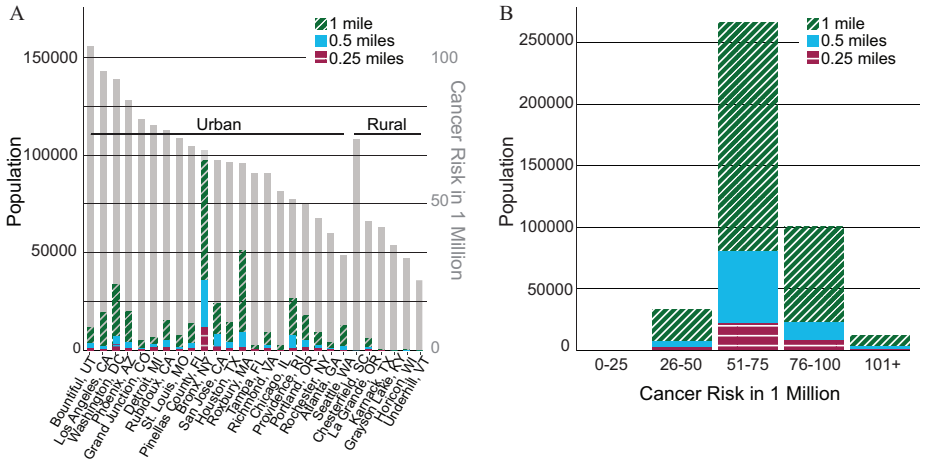

Figure 3. Total estimated cancer risk in 1 million from monitored hazardous air pollutants at National Air Toxics Trends Stations (gray bars, right-hand *y*-axis) and the population levels within a 0.25-, 0.5-, and 1-mi radius for (A) each monitored site and (B) grouped based on total cancer risk (bars are cumulative). Summary data are shown in Tables S2 and S3.

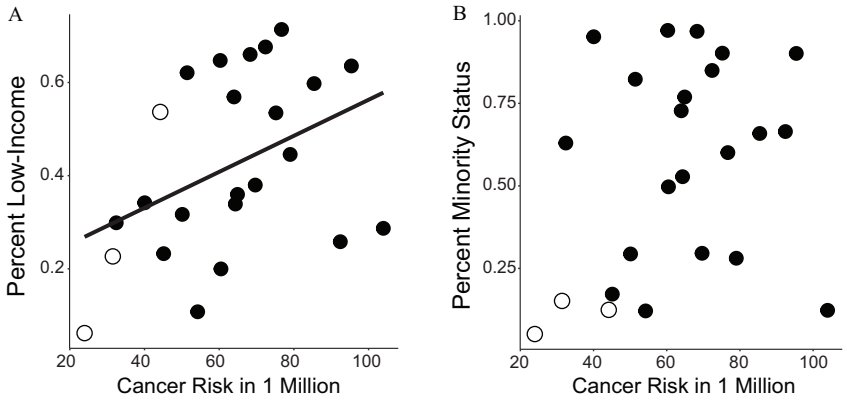

Figure 4. Scatterplot of the relationship between estimated cancer risk in 1 million at NATTS and percent of the population within 1-mi of the monitor that is (A) low income (linear regression: $R^2 = 0.13$, $p = 0.04$, $n = 24$) and (B) minority status (linear regression: $R^2 = 0.04$, $p = 0.19$, $n = 24$). Open circles represent rural NATTS, closed circles represent urban NATTS. Note: Three of the six rural sites were excluded from this analysis. Summary data are shown in Table S4. NATTS, National Air Toxics Trends Stations.

beryllium in Rochester, New York, and methylene chloride in Providence, Rhode Island, also showed statistically significant increases from 2013 to 2017 (Figure 6; Excel Table S5). Each of these HAPs contributed less than 0.02% to the total 5-y cancer risk estimate at the respective site, with the exception of arsenic in Phoenix, which constituted 3.1% of the total estimated cancer risk. In contrast, there were 38 site–chemical combinations that had statistically significant decreasing concentrations over time. The PAH fluoranthene showed decreasing trends at the most sites (seven sites), whereas acenaphthylene, benzo(*b*)fluoranthene, benzo[*ghi*]perylene, naphthalene, and cadmium all decreased at three sites each. The sites with the most HAPs showing statistically significant decreasing trends were Grand Junction and Bountiful with 6 and 5 HAPs, respectively (Figure 6; Excel Table S5).

Covariance Patterns between HAP Concentrations

Using the 5-y average estimated cancer risk, we used hierarchical clustering to examine patterns of covariance between HAP at urban and rural NATTS (Figure 7). For urban sites, we note two primary clusters (Figure 7A; Excel Table S6) acenaphthene, 9h-fluorene, fluoranthene, trichloroethylene, tetrachloroethylene, and naphthalene were positively correlated among themselves (red; Figure 7A; Excel Table S6). Similarly, certain PAHs, including chrysene, benzo(*b*)fluoranthene, indeno[1,2,3-*cd*]pyrene, benzo(*a*)pyrene, perylene, benzo(*k*)fluoranthene, benzo(*e*)pyrene, and benzo(*a*)anthracene were high positively correlated among themselves, falling also within a large, less tightly associated cluster (Figure 7A; Excel Table S6). For rural NATTS (limited to six sites), we point to three large clusters (Figure 7B; Excel Table S7). One cluster contained the PAHs chrysene, benzo(*b*)fluoranthene, benzo(*a*)anthracene, acenaphthylene, benzo(*a*)pyrene, indeno[1,2,3-*cd*]pyrene, and benzo(*e*)pyrene, as well as the VOCs ethylbenzene, methylene chloride, and tetrachloroethylene (Figure 7B; Excel Table S7). A second cluster was composed of the PAHs naphthalene, fluoranthene, acenaphthene, and 9H-fluorene, as well as the VOC benzene (Figure 7B; Excel Table S7). Finally, an additional robust cluster included the VOC *p*-dichlorobenzene and the PM-speciated metals nickel, beryllium, and cadmium (Figure 7B; Excel Table S7).

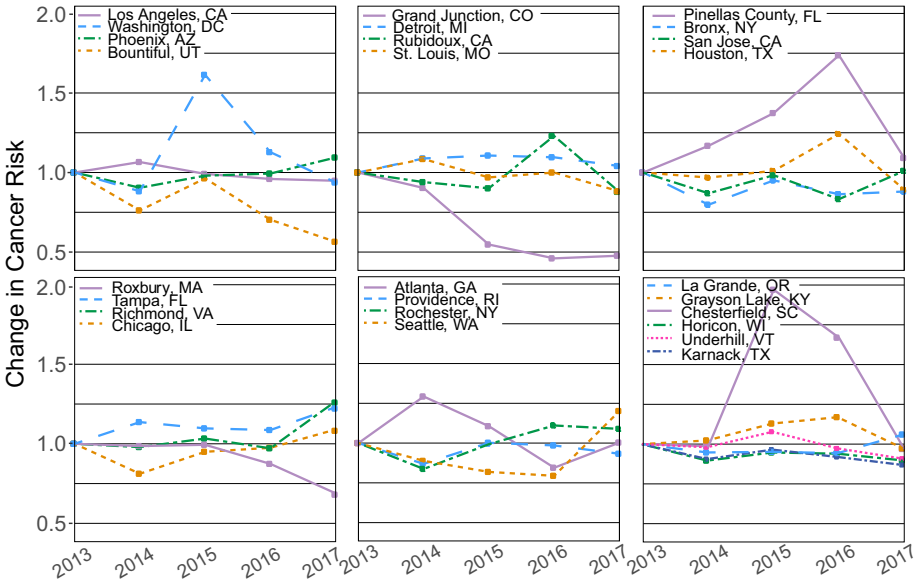

Figure 5. Trends in estimated cancer risk based on the annual average for each National Air Toxics Trends Station from 2013 to 2017. For each site, change is shown as relative to cancer risk based on 2013 annual average hazardous air pollutant concentrations. Summary data are shown in Table S5.

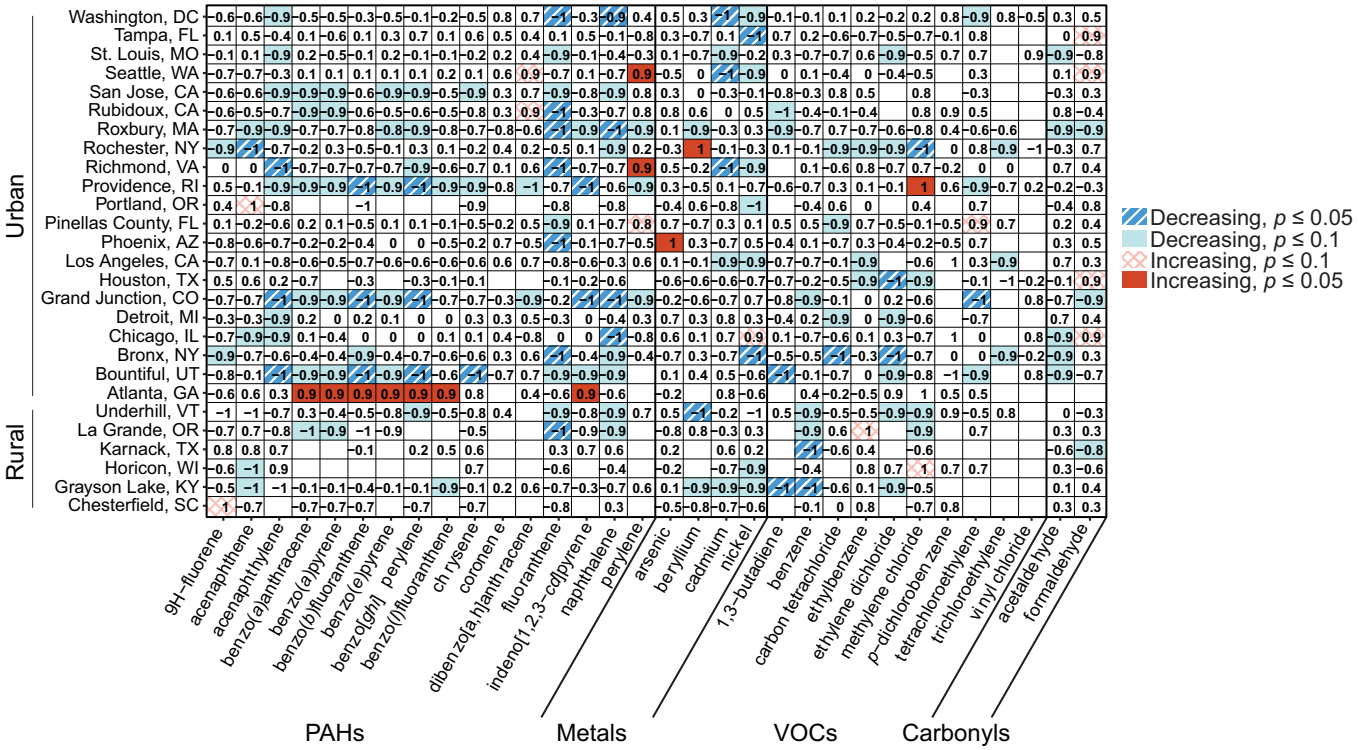

Figure 6. Spearman's rank correlation coefficients representative of changes in concentrations of hazardous air pollutants at National Air Toxics Trends Stations from 2013 to 2017. Only pollutants measured in at least 30% of sites are shown. Dark red = increase at $p \le 0.05$; Light red = increase at $p \le 0.10$; Dark blue = decrease at $p \le 0.05$; Light blue = decrease at $p \le 0.10$. Summary data are shown in Excel Table S5.

Comparison with Modeled Cancer Risk Estimates at the Census Tract

We compared cancer risk estimates in 2014 based on NATTS monitoring data with the modeled estimates of cancer risk at the corresponding census tract from 2014 NATA (Figure 8A; Table S6). For 24 of the 27 locations, the average cancer risk estimate at the NATTS monitor exceeded that of the NATA estimate for 2014. On average, the monitored estimates of cancer risk were 40% higher than the modeled estimates presented in NATA. Next, we compared 2014 NATA exposure and ambient concentrations of formaldehyde and found minimal difference between the two NATA concentration estimates (<2%; Figure S1; Table S7). In contrast, the NATTS measured concentrations of formaldehyde exceeded the NATA census tract exposure concentrations for 24 out of 26 locations (Figure S1; Table S7). Note, an annual average value for formaldehyde was not available in the ambient monitoring archive for the Atlanta NATTS site in 2014.

Discussion

The U.S. EPA report "Our Nation's Air" shows changes in concentrations of HAPs from 2003 to 2019 (U.S. EPA 2020c). This long-term view of trends shows that levels of most air toxics monitored at NATTS have been in decline, likely reflecting the implementation of control strategies required by the 1990 amendments to the Clean Air Act (U.S. EPA 2017). Here, we evaluated a more recent snapshot in time (2013 to 2017) to examine spatial and temporal trends in total cancer risk from concentrations of HAPs measured at NATTS. This approach weights the chemicals driving total estimated cancer risk based on their carcinogenic potency (i.e., UREs) and can point to priority pollutants. We found that no sites had statistically significant changes in total estimated cancer risk over time, though four sites showed trends ($p \le 0.1$) of decreasing risk, including Bountiful, Grand Junction, Los Angeles, and Roxbury. Although cancer risk at most other sites remained relatively consistent, there were notable peaks in estimated cancer risk for three NATTS sites, Washington, DC; Pinellas County; and Chesterfield, primarily corresponding to changes in formaldehyde concentrations and potentially related to atmospheric variability (Lui et al. 2017). These fluctuations in carcinogenic pollution further point to the utility of this analysis. That is, if cancer risk is regularly estimated at monitors such as these, the results can be used to investigate potentially new or increasing levels of existing carcinogenic air pollution and if necessary, to implement strategies to potentially lower the risk to the nearby population.

For pollutant-specific trends, our analysis showed that 38 site-HAP combinations decreased significantly, whereas 12 site-HAP combinations increased from 2013 to 2017. Further reflecting overall reductions in cancer risk, Grand Junction and Bountiful had the greatest number of significantly decreasing HAPs. Across sites, the PAH fluoranthene decreased at the most sites. Traffic-related fuel combustion, primarily from diesel engines, is a major source of fluoranthene and of many of the PAHs (Jia and Batterman 2010; Schauer et al. 2003). The pattern of decreasing concentrations across both urban and rural sites may reflect improvements in diesel engine technology (Liu et al. 2017). In contrast, we identified 12 HAPs with increasing concentrations, 7 of which were in Atlanta. It is important to note that although increases in the concentration of these HAPs were statistically significant over the 5-y period, the levels of each remain low and contribute a small fraction to total estimated cancer risk at each site.

Formaldehyde and benzene were the top two drivers of estimated cancer risk from monitored HAPs across the country, followed by acetaldehyde at urban sites and carbon tetrachloride at rural sites. The carbonyl compounds formaldehyde and

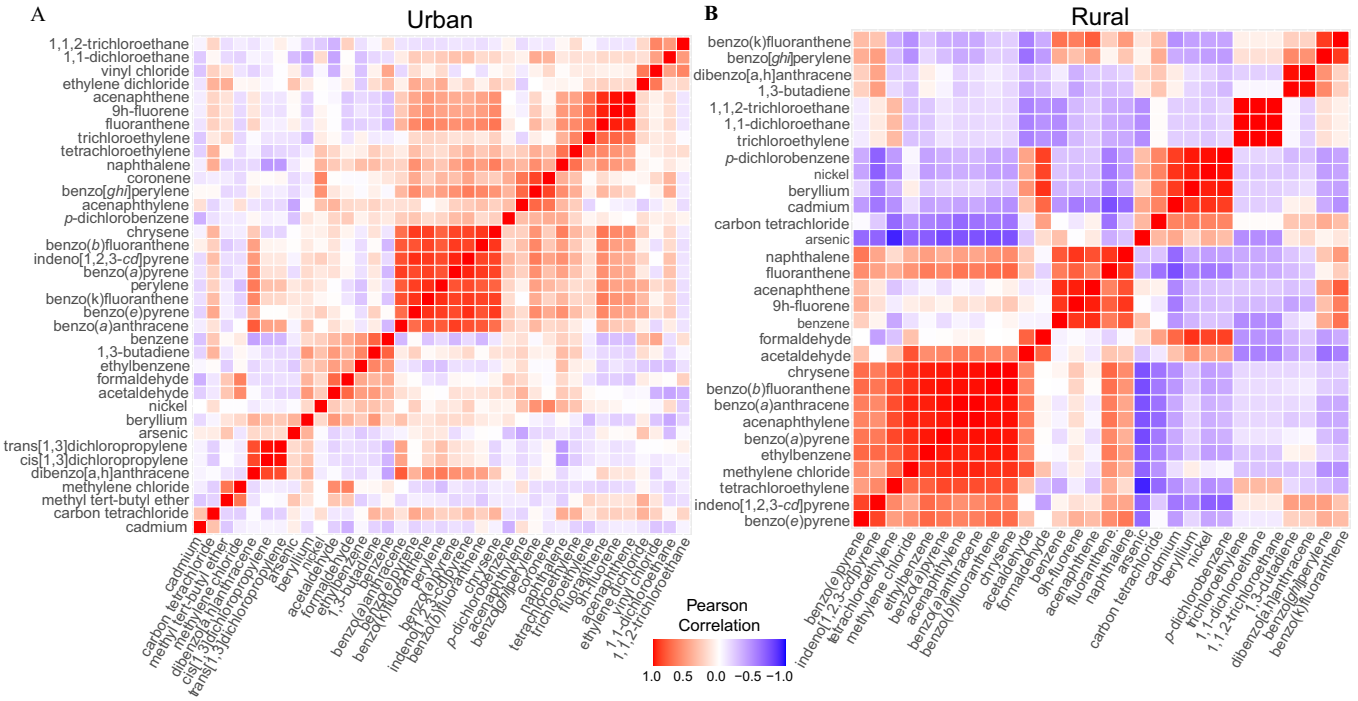

Figure 7. Hierarchically clustered correlation matrices showing the covariance patterns between the 5-y average concentrations of select hazardous air pollutants for (A) urban ($n = 21$) and (B) rural ($n = 6$) National Air Toxics Trends Stations. Only pollutants measured at more than 75% of sites were included. Red = positive correlation; Blue = negative correlation. Summary data are shown in Excel Tables S6 and S7.

acetaldehyde are highly reactive, and their main source is secondary formation in the atmosphere, specifically atmospheric oxidation of biogenic isoprene and oxidation of hydrocarbons, respectively (Millet et al. 2010; Zhu et al. 2017). Based on the national average from the 2014 NATA, the main contributors to primary formaldehyde risks in the United States are biogenics emitted from vegetation, fires (sum of wildfires, prescribed and agricultural), and residential wood combustion. Primary sources contribute approximately 19% of the total formaldehyde emissions, with secondary formation contributing approximately 74% of the total (U.S. EPA 2018c). For benzene, which is not secondarily formed, the main risk contributors are nondiesel light-duty engines, residential wood combustion, and nonroad recreational vehicles. The main contributors of primary acetaldehyde are biogenics, wild and prescribed fires, and nondiesel light-duty vehicles (U.S. EPA 2018c). For carbon tetrachloride, a stable and long-range transport pollutant, nearly 100% of the risk is from background, which was simulated from NATA modeling using remote monitored data as boundary conditions. All the above HAPs meet the regulatory definition of VOC and react with oxides of nitrogen in the presence of sunlight to produce ozone. Tropospheric ozone is a criteria air pollutant and the main component in photochemical smog (U.S. EPA 2020d). The health effects associated with ozone exposure are well-established (U.S. EPA 2020d); thus public health risks from elevated levels of these VOCs include not only increased cancer risk estimated here, but also respiratory and cardiovascular risks related to ambient exposure to ozone.

Although the U.S. EPA does not set a predefined threshold of acceptable risk for HAPs, it is generally presumed that the upper limit of acceptable risk is about 100 in 1 million lifetime cancer risk (U.S. EPA 1999). Based on the 5-y average from 2013 to 2017 for included HAPs, only one site, Bountiful, exceeded this benchmark. It is notable, however, that the annual average cancer risk estimate we calculated for this site decreased from 130 in 1 million in 2013 to 73 in 1 million in 2017. In the 2014 NATA, the census tract–level risk at this site was estimated as 20 in 1 million (U.S. EPA 2018c). The difference in these two risk estimates illustrates the need for multiple tools and could arise for multiple reasons (in addition to the general differences between monitored and modeled estimates discussed below). For example, the risk at Bountiful as calculated in our analysis of monitoring data could potentially reflect the atmospheric inversion that occurs in Utah, in which a layer of warm air traps the colder air below it, allowing for air pollutants to accumulate (Utah DEQ 2020). This inversion may not be well captured at the 12-km grid resolution used in NATA (U.S. EPA 2018e) and could, in part, account for the 5-times lower cancer risk estimate in NATA.

An additional six sites had total cancer risk that ranged between 75 in 1 million and 100 in 1 million, including Los Angeles; Washington, DC; Phoenix; Grand Junction; Detroit, Michigan; and Rubidoux, California. Based on an examination of population levels near the monitors, we found that the highest number of people reside near monitors with cancer risk between 50–75 in 1 million, followed by 75–100 in 1 million. For all sites, formaldehyde had the greatest contribution to total estimated cancer risk. Acrylonitrile also substantially contributed to estimated cancer risk at some sites, including Washington, DC; Grand Junction; Pinellas County; and Tampa, Florida. Acrylonitrile is most commonly emitted from stationary point sources, such as chemical plants, and because it breaks down quickly it is typically only measured near the source (Zoroufchi Benis et al. 2016). Of note, it is possible that some measurements of acrylonitrile can be artificially high due to potential contamination of the collection system (U.S. EPA 2018f).

Urban areas, where HAP sources tend to be more concentrated, have been reported to have poorer air quality in comparison with rural areas (Strosnider et al. 2017). Indeed, we found that the average estimated cancer risk in urban sites from HAPs was 67 in 1 million in comparison with 42 in 1 million at rural NATTS. This result is consistent with general overall higher cancer incidence in urban compared with rural areas. However, the opposite pattern has

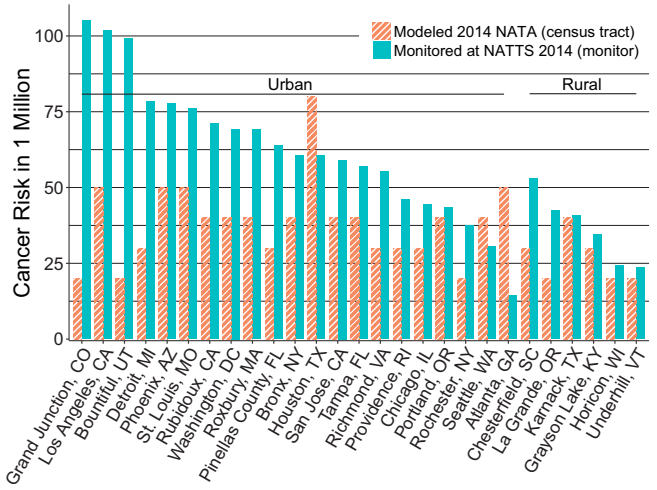

Figure 8. Comparison of 2014 NATA census tract modeled cancer risk estimates to the corresponding cancer risk estimate at the NATTS monitor in 2014. Note: The 2014 annual average formaldehyde concentration was not available for the Atlanta, Georgia NATTS monitor. Summary data are shown in Tables S6 and S7. NATA, National Air Toxics Assessment; NATTS, National Air Toxics Trends Stations.

previously been observed for cancer mortality, whereby mortality is higher in rural areas compared with urban areas (Henley et al. 2017). This discrepancy may be due in part to a higher prevalence of lifestyle factors in rural areas that may modify cancer risk and mortality due to HAP exposures (Henley et al. 2017). For example, there is a higher prevalence of cigarette smoking, physical inactivity, and obesity in rural areas (Matthews et al. 2017), in addition to lack of access to cancer screening and care (Meilleur et al. 2013). Indicators of social vulnerability have been captured by tools such as the Centers for Disease Control and Prevention's Social Vulnerability Index and the U.S. EPA's EJSCREEN (ATSDR 2020). Here, we analyzed demographic indicators from EJSCREEN, which provided the finest spatial resolution (i.e., block group level). We found no relationship with minority status but a positive correlation between percent low income and the total estimated cancer risk from HAPs, suggesting that communities with higher concentrations of HAPs may be further disadvantaged by being less well-equipped to cope with external stressors such as air pollutants. That said, it is important to note that in this analysis we are using the estimated cancer risk at a NATTS monitor as a surrogate for population exposure. Therefore, the potential cancer risk of these groups from exposure to HAPs may be higher or lower.

An exploratory comparison of hierarchically clustered correlation matrices showing covariance patterns among HAPs suggests potential differences in HAP sources between urban and rural sites. We note a similar cluster within both urban and rural sites that contained six shared PAHs. An interesting finding is that within the rural matrix only, the VOCs ethylbenzene, methylene chloride, and tetrachloroethylene were also tightly associated with this cluster. Based on NATA, methylene chloride and tetrachloroethylene share the same primary sources of solvents and coatings, stationary points, and waste disposal (U.S. EPA 2018c). Although the main source of ethylbenzene is from vehicles, these other sources are among the top ten contributors. It may be that with greater distance to roads and vehicles in the rural areas these other sources gain importance. Notably, given that there are only 6 rural vs. 21 urban sites, there was considerably less statistical robustness in the former.

Characterizing cancer risk from monitored concentrations of HAPs is a valuable complement to the screening-level cancer risk estimates derived by modeling approaches. To further illustrate this point, we compared the cancer risk estimates from 2014 NATTS monitoring data to the 2014 NATA modeled cancer risk estimates at the corresponding census tracts. We found that, on average, the monitored cancer risk estimates exceeded those of the modeled by approximately 40%. Several factors may account for this discrepancy. First, most NATTS-based estimates are at a single geographic point in an urban area. If these monitors were located among the higher sites of cancer risk within the entire census tract, we would expect the aggregated modeled cancer risk from NATA for the entire tract to be lower. This effect would likely be more pronounced in locations where the census tract is large but contains only a few sources concentrated to a single geographic area. More specifically, in NATA, ambient concentrations modeled at the block level are population weighted to the census tract. This results in an averaging of higher point concentrations. In addition, previous work that compared monitored formaldehyde concentrations to modeled concentrations using the hybrid approach employed in NATA found that the model underpredicted formaldehyde by approximately 30% (Scheffe et al. 2016; U.S. EPA 2018e), consistent with our observations. Given that formaldehyde is the primary driver of estimated cancer risk, an underprediction of this HAP by the model may account for an appreciable portion of the difference between the NATTS and NATA estimates. In contrast, for three sites the modeled cancer risk was higher than the monitored. This finding could be due to a variety of reasons, including missing monitored pollutants (e.g., formaldehyde in Atlanta) and/or the location of the NATTS monitor relative to sources in the area. Another difference between modeled and monitored cancer risk estimates is in the assumptions regarding exposure. In our analysis of NATTS data, we used concentration at the monitor as a surrogate for exposure. In contrast, NATA applies an exposure model to concentrations at the tract before estimating cancer risk (U.S. EPA 2018e). However, our results demonstrated little difference between ambient and exposure concentrations for formaldehyde; thus it is unlikely that differences between the monitored and modeled cancer risk estimates are driven largely by differences in exposure assumptions. Notably though, a more detailed exposure analysis could show differences up to 25% for highly reactive pollutants such as formaldehyde (e.g., U.S. EPA 2001). Taken together, this comparison suggests that NATA is a valuable tool to estimate risk at large spatial scales but that standardized monitoring approaches are also needed to characterize risk within communities.

There are also several uncertainties that apply to characterizing cancer risk based on monitoring data. It is important to note that our approach estimates cancer risk based on UREs, which are designed to be associated with a lifetime (70 y) of exposure. Applying these values to shorter durations may not accurately reflect individual-level risk. Moreover, as mentioned above, we used the levels of individual carcinogens measured at monitors as a surrogate for human exposure and carcinogenic risk without considering time activity patterns, most notably, time spent indoors. Although indoor air levels of HAPs are typically reflective of outdoor levels, there can be variation in this based on several factors, such as the class of HAP, the ventilation system and building design, and proximity to roadways and other sources (Turpin et al. 2007). In some cases, the indoor environment can serve as a sink for air pollutants (Tong et al. 2016). Overall, this assumption likely leads to an overestimate of carcinogenic health risk in some locations. An additional uncertainty in our analyses is the assumption of additivity of risk, rather than synergy or antagonism. Last, there are a limited number of NATTS sites, particularly within the West North Central division of the Midwest, thus representing an important data gap.

Several factors in our analyses may lead to an underestimation of cancer risk in many locations. Notably, the approach used

for estimating total cancer risk is completely dependent on the number and potency of carcinogens monitored at each NATTS. In our analyses, on average over 70 HAPs were measured across sites, with 41 of these identified as carcinogenic. Of the 187 HAPs listed under the Clean Air Act, 71 currently have a URE, and there may be additional HAP that are carcinogenic but do not yet have a defined URE. Similarly, there may also be other carcinogenic air pollutants not listed as HAPs. Thus, our results are not a full account of cancer risk from air pollutants. Furthermore, not only does the number of HAPs measured at each site affect risk, but cancer risk is also dependent on the carcinogenic potency of the HAPs measured at each site. That is, any two or more sites may measure the same number of HAPs, but one site may have a lower estimated carcinogenic risk because it might not measure carcinogens present with relatively higher URE values. An underestimation of risk at some sites may have also occurred by our exclusion of carcinogenic HAPs when annual means were significantly affected by NDs. In addition, if more than 80% of values used to compute an annual mean were NDs, we treated the annual mean as zero. Therefore, given the uncertainties described above, when considering the results of individual sites and when making comparisons between sites, there should be caution with regard to forming large-scale conclusions.

Overall, by examining a recent snapshot in time (2013–2017), we found that total estimated cancer risk from HAPs mostly remained unchanged, though four sites showed trends of decreasing risk over the 5-y period examined. However, we still identified areas that are at or near the U.S. EPA presumed upper limit of acceptability, suggesting the need for further investigation at certain locations. To gain further insight into the health effects from carcinogenic HAPs and to aid in identifying priority locations and pollutants, future studies could aim to overlay cancer incidence data with estimated cancer risk from monitored HAPs. Furthermore, additional analyses could be used to examine interactions between HAPs and other environmental pollutants to determine whether there is enhanced or reduced carcinogenicity from mixtures of pollutants, as well as the role of atmospheric transformations. This multipronged approach that includes separate analysis of cancer risk based on both an emissions inventory and on monitored values, potentially overlaid with incidence data, would provide insight into strategies and actions to mitigate the cancer risk to public health from ambient air toxics. Finally, it is important to note that although this manuscript addresses the potential for carcinogenic risk, many HAPs are also of concern because they can potentially contribute to noncancer adverse outcomes. Thus, even at NATTS sites that may have relatively low carcinogenic risk, the potential for appreciable adverse noncancer outcomes exists.

Acknowledgments

The authors thank J. Reyes, J. Nichols, and J. Vandenberg for help in improving the manuscript. This manuscript has been reviewed by the U.S. EPA and approved for publication. Approval does not necessarily signify that the contents reflect the views or opinions of the U.S. EPA, nor does mention of trade names or commercial products constitute endorsement or recommendation for use.

References

ATSDR (Agency for Toxic Substances and Disease Registry). 2020. CDC social vulnerability index. https://www.atsdr.cdc.gov/placeandhealth/svi/index.html [accessed 20 October 2020].

Henley SJ, Anderson RN, Thomas CC, Massetti GM, Peaker B, Richardson LC. 2017. Invasive cancer incidence, 2004–2013, and deaths, 2006–2015, in nonmetropolitan and metropolitan counties—United States. MMWR Surveill Summ 66(14):1–13, PMID: 28683054.

Jia CR, Batterman S. 2010. A critical review of naphthalene sources and exposures relevant to indoor and outdoor air. Int J Environ Res Public Health 7(7):2903–2939, PMID: 20717549, https://doi.org/10.3390/ijerph7072903.

Liu B, Xue ZQ, Zhu XL, Jia CR. 2017. Long-term trends (1990–2014), health risks, and sources of atmospheric polycyclic aromatic hydrocarbons (PAHs) in the US. Environ Pollut 220(Pt B):1171–1179, PMID: 27847130, https://doi.org/10.1016/j.envpol.2016.11.018.

Lui KH, Ho SSH, Louie PKK, Chan CS, Lee SC, Hu D, et al. 2017. Seasonal behavior of carbonyls and source characterization of formaldehyde (HCHO) in ambient air. Atmos Environ 152:51–60, https://doi.org/10.1016/j.atmosenv.2016.12.004.

Matthews KA, Croft JB, Liu Y, Lu H, Kanny D, Wheaton AG, et al. 2017. Health-related behaviors by urban-rural county classification—United States, 2013. MMWR Surveill Summ 66:1–8, PMID: 28151923, https://doi.org/10.15585/mmwr.ss6605a1.

McCarthy MC, O'Brien TE, Charrier JG, Hafner HR. 2009. Characterization of the chronic risk and hazard of hazardous air pollutants in the United States using ambient monitoring data. Environ Health Perspect 117(5):790–796, PMID: 19479023, https://doi.org/10.1289/ehp.11861.

Meilleur A, Subramanian SV, Plascak JJ, Fisher JL, Paskett ED, Lamont EB. 2013. Rural residence and cancer outcomes in the United States: issues and challenges. Cancer Epidemiol Biomarkers Prev 22(10):1657–1667, PMID: 24097195, https://doi.org/10.1158/1055-9965.EPI-13-0404.

Millet DB, Guenther A, Siegel DA, Nelson NB, Singh HB, de Gouw JA, et al. 2010. Global atmospheric budget of acetaldehyde: 3-D model analysis and constraints from in-situ and satellite observations. Atmos Chem Phys 10(7):3405–3425.

Schauer C, Niessner R, Pöschl U. 2003. Polycyclic aromatic hydrocarbons in urban air particulate matter: decadal and seasonal trends, chemical degradation, and sampling artifacts. Environ Sci Technol 37(13):2861–2868, PMID: 12875387, https://doi.org/10.1021/es034059s.

Scheffe RD, Strum M, Phillips SB, Thurman J, Eyth A, Fudge S, et al. 2016. Hybrid modeling approach to estimate exposures of hazardous air pollutants (HAPs) for the national air toxics assessment (NATA). Environ Sci Technol 50(22):12356–12364, PMID: 27779870, https://doi.org/10.1021/acs.est.6b04752.

Stewart MJ, Hirtz J, Woodall GM, Weitekamp CA, Spence K. 2019. A comparison of hourly with annual air pollutant emissions: implications for estimating acute exposure and public health risk. J Air Waste Manag Assoc, PMID: 30870104, https://doi.org/10.1080/10962247.2019.1593261.

Strosnider H, Kennedy C, Monti M, Yip FY. 2017. Rural and urban differences in air quality, 2008–2012, and community drinking water quality, 2010–2015–United States. MMWR Surveill Summ 66:1–10, PMID: 28640797, https://doi.org/10.15585/mmwr.ss6613a1.

Strum M, Scheffe R. 2016. National review of ambient air toxics observations. J Air Waste Manag Assoc 66(2):120–133, PMID: 26230369, https://doi.org/10.1080/10962247.2015.1076538.

Tong ZM, Chen YJ, Malkawi A, Adamkiewicz G, Spengler JD. 2016. Quantifying the impact of traffic-related air pollution on the indoor air quality of a naturally ventilated building. Environ Int 89–90:138–146, PMID: 26829764, https://doi.org/10.1016/j.envint.2016.01.016.

Turpin BJ, Weisel CP, Morandi M, Colome S, Stock T, Eisenreich S, et al. 2007. Relationships of Indoor, Outdoor, and Personal Air (RIOPA): part II. Analyses of concentrations of particulate matter species. Res Rep Health Eff Inst 130 (Pt 2):1–77, PMID: 18064946.

U.S. Census Bureau. 2010. Census, 2010; Census Summary File 1. https://www.census.gov/data/tables/2010/dec/2010-summary-file-1.html [accessed 10 October 2020].

U.S. Census Bureau. 2020a. Poverty Thresholds. https://www.census.gov/data/tables/time-series/demo/income-poverty/historical-poverty-thresholds.html [accessed 4 January 2021].

U.S. Census Bureau. 2020b. American Community Survey (ACS). https://www.census.gov/programs-surveys/acs [accessed 4 January 2020].

U.S. EPA (U.S. Environmental Protection Agency). 1999. Residual Risk Report to Congress. U.S. Environmental Protection Agency. Report number: EPA-453/R-99-001. Research Triangle Park, NC: U.S. Environmental Protection Agency.

U.S. EPA. 2001. National-Scale Air Toxics Assessment for 1996. EPA-453/R-01-003. Research Triangle Park, NC: U.S. Environmental Protection Agency.

U.S. EPA. 2005. Guidelines for Carcinogen Risk Assessment. EPA/630/P-03/001F. Washington, DC: U.S. Environmental Protection Agency.

U.S. EPA. 2016. Technical Assistance Document for the National Air Toxics Trends Station Program. https://www3.epa.gov/ttnamti1/files/ambient/airtox/NATTS%20TAD%20Revision%203_FINAL%20October%202016.pdf [accessed 8 July 2020].

U.S. EPA. 2017. The Clean Air Act - Highlights of the 1990 Amendments. https://www.epa.gov/clean-air-act-overview/clean-air-act-highlights-1990-amendments [accessed 8 January 2020].

U.S. EPA. 2018a. Download Human Exposure Model (HEM). Toxicity value files. https://www.epa.gov/fera/download-human-exposure-model-hem [accessed 20 January 2021].

U.S. EPA. 2018b. 2014 NATA Map. https://gispub.epa.gov/NATA/ [accessed 5 October 2020].

U.S. EPA. 2018c. 2014 NATA: Assessment Results. https://www.epa.gov/national-air-toxics-assessment/2014-nata-assessment-results [accessed 8 July 2020].
U.S. EPA. 2018d. 2014 National Emissions Inventory report. Washington, DC. https://www.epa.gov/sites/production/files/2017-04/documents/2014neiv1_profile_final_april182017.pdf [accessed 3 February 2021].
U.S. EPA. 2018e. Technical Support Document – EPA's 2014 National Air Toxics Assessment. https://www.epa.gov/sites/production/files/2018-09/documents/2014_nata_technical_support_document.pdf [accessed 8 July 2020].
U.S. EPA. 2018f. 2015–2016 National Monitoring Programs Annual Report. https://www3.epa.gov/ttnamti1/files/ambient/airtox/2015-2016%20NMP%20Report%20508.pdf [accessed 8 July 2020].
U.S. EPA. 2019a. AQS Data Coding Manual. Version 3.7. https://www.epa.gov/sites/production/files/2015-09/documents/aqs_data_coding_manual_0.pdf [accessed 2 February 2020].
U.S. EPA. 2019b. National air toxics trends station work plan template. https://www3.epa.gov/ttn/amtic/files/ambient/airtox/nattsworkplantemplate.pdf [accessed 7 October 2020].
U.S. EPA. 2019c. EJSCREEN Technical Documentation. https://www.epa.gov/ejscreen/technical-documentation-ejscreen [accessed 7 October 2020].
U.S. EPA. 2020a. Compilation and quality assurance (QA) summary report for the phase xiii ambient monitoring archive for hazardous air pollutants (HAPs). https://www3.epa.gov/ttn/amtic/files/toxdata/techmemo2019.pdf.
U.S. EPA. 2020b. Air toxics data: Ambient monitoring archive. Annual average statistics. https://www3.epa.gov/ttnamti1/toxdat.html#data [accessed 2 February 2020].
U.S. EPA. 2020c. Our Nation's Air. https://gispub.epa.gov/air/trendsreport/2020/.
U.S. EPA. 2020d. Integrated Science Assessment (ISA) for Ozone and Related Photochemical Oxidants (Final Report). EPA/600/R-20/012: U.S. Environmental Protection Agency, Washington, DC.
U.S. EPA. 2020e. Health Effects Notebook for Hazardous Air Pollutants. https://www.epa.gov/haps/health-effects-notebook-hazardous-air-pollutants [accessed 7 October 2020].
Utah DEQ (Utah Department of Environmental Quality). 2020. Inversions. https://deq.utah.gov/air-quality/inversions [accessed 18 November 2020].
Zhu L, Jacob DJ, Keutsch FN, Mickley LJ, Scheffe R, Strum M, et al. 2017. Formaldehyde (HCHO) as a hazardous air pollutant: mapping surface air concentrations from satellite and inferring cancer risks in the United States. Environ Sci Technol 51(10):5650–5657, PMID: 28441488, https://doi.org/10.1021/acs.est.7b01356.
Zoroufchi Benis K, Shakerkhatibi M, Yousefi R, Kahforoushan D, Derafshi S. 2016. Emission patterns of acrylonitrile and styrene around an industrial wastewater treatment plant in Iran. Int J Environ Sci Technol 13(10):2353–2362, https://doi.org/10.1007/s13762-016-1053-9.